Extended Abstracts of the 1998 International Conference on Solid State Devices and Materials, Hiroshima, 1998, pp. 90-91

Oxide Thickness Dependence of Hot Carrier Stress Induced Drain Leakage Current Degradation in Thin-Oxide n-MOSFET's

*Tahui Wang, N.K. Zous, L.Y. Huang, C.K. Yeh and T.S. Chao**

Department of Electronics Engineering, National Chiao-Tung University
*National Nano Devices Lab., Hsin-Chu, Taiwan, R.O.C.
Fax: 886-3-5724361, Email:wang@jekyll.ee.nctu.edu.tw

1. Introduction

The reduction of drain leakage current at zero V_{gs} has been a major concern in CMOS device scaling. Hot carrier (HC) stress induced drain leakage current degradation has received much attention recently [1-3]. The HC stress effects on drain leakage current are twofold, interface trap (N_{it}) generation and fixed oxide charge (Q_{ox}) creation. N_{it} can introduce additional drain leakage mechanisms including sequential tunneling current (I_{TAT}), thermionic-field emission current (I_{TF}) and Shockley-Read-Hall generation current (I_{SRH}). The closed-form expressions for these leakage currents were derived in our previous work [1,3] and are shown in Table 1. The Q_{ox} effect on drain leakage degradation is through the modification of the Si surface field. The build-up of negative oxide charge results in an increase of the surface field and thus the enhancement of band-to-band tunneling current (I_{BB}) [4] and the N_{it}-assisted tunneling current I_{TAT}. The Q_{ox}-induced I_{BB} and I_{TAT} degradations are formulated in Eqs.(7) and (8) in Table 1.

Moreover, recent research showed that Q_{ox} generation varies with a gate oxide thickness (t_{ox}) [5,6]. In ultra-thin oxides ($t_{ox} \leq 40Å$), Q_{ox} generation is negligible because trapped oxide charge can easily escape via tunneling. In this work, we intend to compare the HC stress induced drain leakage current degradation characteristics in n-MOSFET's with different oxide thicknesses.

2. Device Characterization

The test devices are 0.35μm n-MOSFET's with source/drain extension. The gate oxide thicknesses are 53Å, 40Å and 30Å. The gate width is 100μm. The devices are subject to maximum substrate current stress at V_{gs}=2V and V_{ds}=4.5V. The pre-stress and post-stress I_d-V_{gs} in a 40Å oxide device are shown in Fig.1. Various drain leakage components at V_{gs}=0V in the stressed device are shown in Fig. 2. I_s is the drain-to-source subthreshold leakage current. ΔI_d is the stress induced leakage current obtained from the difference between the pre-stress and post-stress currents. In calculation, N_{it} is $1.4 \times 10^{12} cm^{-2}$ and ΔL is 400Å to fit the measured data. The dominant leakage mechanism in different ranges of V_{ds} is also indicated in the figure. For example, the dominant leakage current is I_{BB} for $V_{ds} \geq 3.1V$, I_{TAT} for $3.1V \geq V_{ds} \geq 1.8V$ and so forth. Since I_{BB} is affected only by Q_{ox} while I_{TAT} is influenced by both N_{it} and Q_{ox}, we can characterize the N_{it} and Q_{ox} induced degradations separately by measuring I_{BB} and I_{TAT}.

3. Results and Discussion

The drain leakage degradation in two different oxide thickness (30Å and 53Å) devices is measured at V_{ds}=2.5V and V_{gs}=0V. Note that the dominant leakage current at the measurement bias is I_{TAT}. For the purpose of comparison, the I_{TAT}'s in the two devices are normalized to have the same starting point in Fig. 3. The 30Å oxide device shows a power law degradation rate in the entire stress period. The power factor is about 0.4, which reflects the N_{it} growth rate. The I_{TAT} in the 53Å oxide device, however, exhibits a two-stage degradation. In the first stage ($t \leq 10^3$sec), N_{it} is dominant and the degradation follows a power-law dependence. In the second stage, Q_{ox} creation becomes dominant and I_{TAT} shows an accelerated degradation. The modeled results from Eqs.(11) and (13) are shown by the solid lines in the figure. The extracted Q_{ox} power factor is about 0.25. It should be emphasized that although the two devices have the same initial degradation rate, the drain leakage degradation in the thinner oxide device is significantly improved for $t \geq 10^3$sec.

Since I_{BB} is affected by Q_{ox}, measurement of the drain leakage current at V_{ds}=1.5V and V_{gs}=-3V, where I_{BB} is dominant, can be used to monitor oxide charge creation. The results are shown in Fig. 4. I_{BB} is nearly constant in the two devices for $t \leq 10^3$sec, which implies minimal Q_{ox} creation. A slight decline of I_{BB} in this period can be realized due to a small amount of positive oxide charge (or interface charge) creation. For $t \geq 10^3$sec, the I_{BB} in the 30Å oxide device remains constant while the I_{BB} in the 53Å oxide increases drastically. The enhancement of the I_{BB} is well fitted by Eq.(12) with n_2=0.25 (solid line in Fig. 4). Furthermore, our model shows that I_{BB} and I_{TAT} exhibit a bias dependence. The degradation rates are worsened at a smaller surface field. To verify our model, we measure the I_{BB} at three different biases, V_{ds}=1.5V, 2.0V, 2.5V and V_{gs}=-3V. The result is shown in Fig. 5. Apparently, the I_{BB} degradation at V_{ds}=1.5V is most serious, as expected from the model. Finally, we would like to mention that the degradation characteristics in the 40Å oxide device are similar to those in the 30Å oxide device.

4. Conclusion

We have observed a strong oxide thickness dependence of hot carrier stress induced drain leakage degradation in thin-oxide n-MOSFET's. In ultra-thin oxide (≤40Å) devices, the drain leakage degradation is attributed mostly to interface trap generation while in thicker oxide devices the degradation is driven by both interface trap and oxide charge creation. By using a thinner gate oxide (≤40Å), the hot carrier stress induced drain leakage degradation can be much improved.

[1] T. Wang et al., *IEEE T-ED*, Vol. 42, p.738, 1995
[2] A. Frommer et al., *Symp. on VLSI Tech.*, p.164, 1996

[3] T. Wang et al., *SSDM*, p.368, 1997
[4] T.Y. Chan et al., *IEDM Tech. Dig.*, p.721, 1987
[5] H.S. Momose et al., *IEDM Tech. Dig.*, p. 453, 1997
[6] M. Yoshida et al., *IEDM Tech. Dig.*, p. 254, 1985
[7] T. Wang et al., *Symp. on VLSI Tech.*, p. 232, 1996

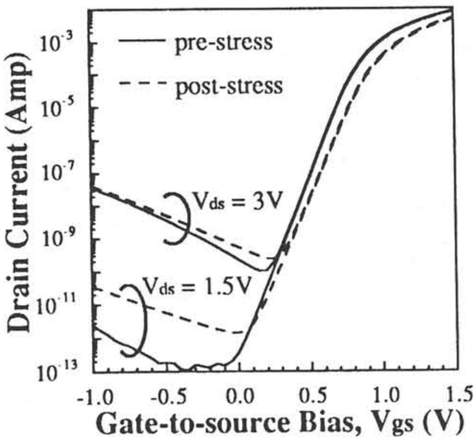

Fig.1 Pre-stress and post-stress Id-Vgs. Stress time is 3000 sec.

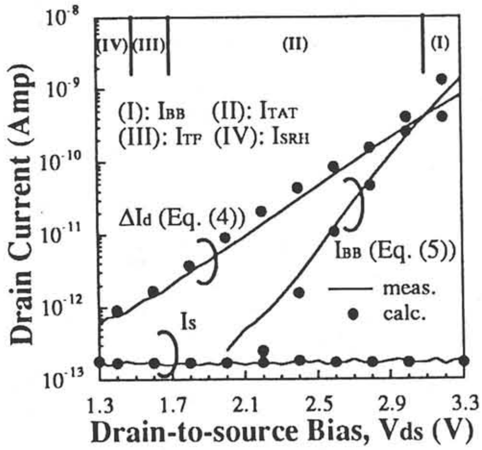

Fig. 2 Various drain leakage current components at Vgs=0V. The dominant drain leakage current in different ranges of Vds is indicated.

Table. 1 Mechanisms of hot carrier stress induced drain leakage current degradation. Te and Th in Eqs. (1-4) denote electron and hole tunneling rates [3]. Ge and Gh represent electron and hole thermionic emission rates. ΔL is the length of the Nit region. Bit in Eq. (6) is defined in [1]. E is the Si surface field.

(a) Nit -assisted drain leakage currents

$$I_{TAT}=qW\int_{\Delta L}\int_{bandgap} N_{it}\frac{T_eT_h}{G_e+T_e}\,d\varepsilon\,dx \qquad (1)$$

$$I_{TF}=qW\int_{\Delta L}\int_{bandgap} N_{it}\frac{T_eG_h+T_hG_e}{G_e+T_e}\,d\varepsilon\,dx \qquad (2)$$

$$I_{SRH}=qW\int_{\Delta L}\int_{bandgap} N_{it}\frac{G_eG_h}{G_e+T_e}\,d\varepsilon\,dx \qquad (3)$$

$$\Delta I_d=I_{SRH}+I_{TF}+I_{TAT}=qW\int_{\Delta L}\int_{bandgap} N_{it}(G_e+T_e)\,d\varepsilon\,dx \qquad (4)$$

(b) Qox induced drain leakage degradation

$$I_{BB}\propto E\exp(-B/E) \qquad (5)$$

$$I_{TAT}\propto N_{it}\exp(-B_{it}/E) \quad \text{(Ref[1])} \qquad (6)$$

$$I_{BB}(Q_{ox}) \sim I_{BB}(0)\exp(\alpha_{BB}Q_{ox}) \quad \text{(Ref[7])} \qquad (7)$$

$$I_{TAT}(Q_{ox}) \sim I_{TAT}(0)\exp(\alpha_{TAT}Q_{ox}) \qquad (8)$$

$$\alpha_{BB}=B/(\epsilon_{si}E^2) \qquad \alpha_{TAT}=B_{it}/(\epsilon_{si}E^2)$$

(c) stress time dependence

$$N_{it}=A_1t^{n1} \qquad Q_{ox}=A_2t^{n2} \qquad (9)$$

(i) Nit dominant

$$I_{BB}(t) \sim \text{constant} \qquad (10)$$

$$I_{TAT}(t) \propto N_{it} \propto t^{n1} \qquad (11)$$

(ii) Qox dominant

$$I_{BB}(t) \propto \exp(\alpha_{BB}A_2t^{n2}) \qquad (12)$$

$$I_{TAT}(t) \propto \exp(\alpha_{TAT}A_2t^{n2}) \qquad (13)$$

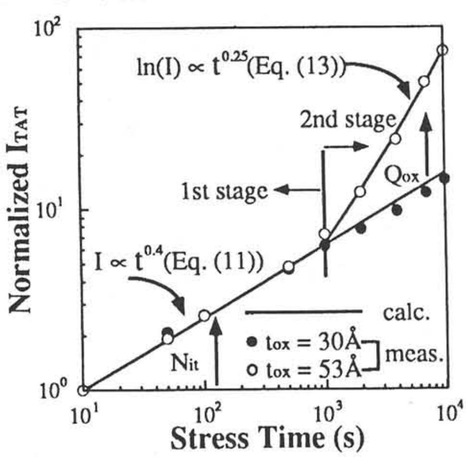

Fig. 3 Stress time dependences of the I_{TAT} measured at Vds=2.5V and Vgs=0V in 30Å oxide and 53Å oxide devices. The two I_{TAT}'s are normalized to have the same initial value.

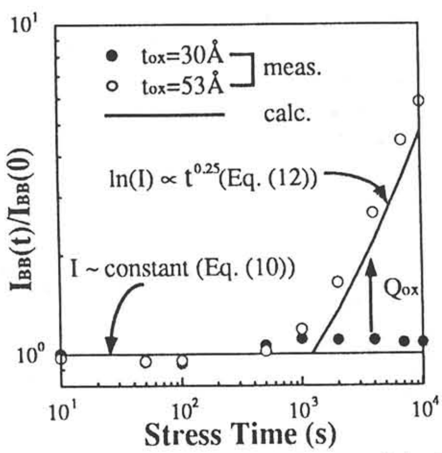

Fig. 4 Stress time dependences of the I_{BB} measured at Vds=1.5V and Vgs=-3.0V in 30Å oxide and 53Å oxide n-MOSFET's.

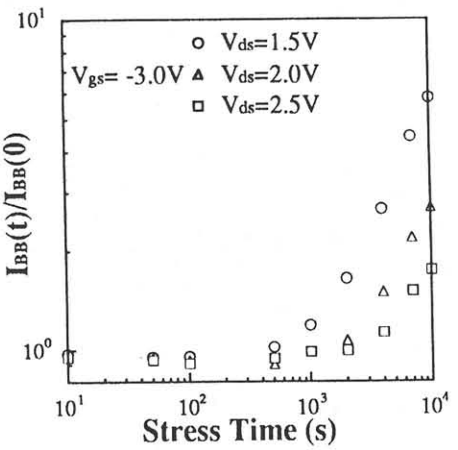

Fig. 5 The I_{BB} measured at three different biases, Vds=1.5V, 2.0V, 2.5V and Vgs=-3.0V in the 53Å n-MOSFET.